Cocrystallization of Organometallic Clusters: Homo- and Heteromolecular Crystals of $Ru_6C(CO)_{14}(\eta^6\text{-}C_6H_4Me_2)$ and $Ru_6C(CO)_{11}(\eta^6\text{-}C_6H_4Me_2)_2$

Dario Braga,* Fabrizia Grepioni, Caroline M. Martin, and Emilio Parisini

Dipartimento di Chimica G. Ciamician, Università di Bologna, Via Selmi 2, 40126 Bologna, Italy

Paul J. Dyson and Brian F. G. Johnson*

Department of Chemistry, The University of Edinburgh, West Mains Road, Edinburgh EH9 3JJ, U.K.

Received November 1, 1993®

The molecular structure of $Ru_6C(CO)_{11}(\eta^6\text{-}C_6H_4Me_2)_2$ (**2**) has been established by the single crystal X-ray diffraction method in its crystalline form **B**. The species has also been found to cocrystallize with $Ru_6C(CO)_{14}(\eta^6\text{-}C_6H_4Me_2)$ (**1**), and the structure of the heteromolecular cocrystal **C** has been determined. A homomolecular crystal of **1** (crystal **A**) had been discovered previously. The mono- and bis(xylene) derivatives in their homo- and heteromolecular crystals have been compared in terms of molecular and crystal structure, intermolecular interlocking, and packing potential energies. Crystal **B**, containing only molecules of type **2**, is monoclinic, space group Pn, a = 10.242(3) Å, b = 14.047(6) Å, c = 11.242(2) Å, β = 106.15(2)°, V = 1553.6(9) Å^3, Z = 4. Cocrystal **C**, formed by **1** and **2**, is triclinic, space group $P\bar{1}$, a = 9.852(4) Å, b = 10.444(9) Å, c = 32.320(10) Å, α = 95.65(6)°, β = 92.03(4)°, γ = 115.29(4)°, V = 2981(3) Å^3, Z = 2 on each molecular unit. It has been shown that a precise relationship exists between the crystal structures of the homomolecular crystals **A** and **B** and that of the heteromolecular crystal **C**, the last being essentially formed by bimolecular layers similar to those present in the separate crystals. The three crystal forms also compare strictly in terms of packing efficiency and crystal cohesion.

Introduction

Cocrystallization of organic compounds is a common phenomenon,[1] often of commercial importance. In organometallic chemistry many anion–cation pairs and, to a lesser extent, pairs of conformational isomers in the same crystal and polymorphs have been recognized.[2] However, we are not aware of any examples in which two different neutral cluster molecules have cocrystallized. In this paper we want to describe the first case of cocrystallization of two neutral organometallic species, $Ru_6C(CO)_{14}(\eta^6\text{-}C_6H_4Me_2)$[3] and $Ru_6C(CO)_{11}(\eta^6\text{-}C_6H_4Me_2)_2$, which retain in the cocrystal the same packing features shown by the two molecules in their separate crystals.

It is worth describing here some of the general features we have observed in the past, concerning the packing of mono- and bis(arene) cluster derivatives of the hexaruthenium carbido carbonyl cluster $Ru_6C(CO)_{17}$.[4a,b] The main packing interaction in this binary carbonyl cluster consists of "trains" of molecules, head-to-tail linked *via* insertion of the bridging carbonyl belonging to one molecule into a tetragonal cavity formed by four CO groups on a neighboring molecule.[4b] Although this interaction is still present in the mono(arene) derivatives $Ru_6C(CO)_{14}(\eta^6\text{-arene})$, another important feature in their packing is the tendency shown by the arene ligands to group in layers forming "ribbons" throughout the lattice, while the CO groups interact with each other.[5] This suggests that molecules arrange themselves to optimize the interlocking between the flat arenes, while keeping the protuberant CO groups together. This is exactly what is observed in the bis(arene) complexes, where the packing features do not change significantly among the three observed structural types, *i.e.* *cis*-$Ru_6C(CO)_{11}(\eta^6\text{-arene})_2$, *trans*-$Ru_6C(CO)_{11}(\eta^6\text{-arene})_2$, and $Ru_6C(CO)_{11}(\eta^6\text{-arene})(\mu_3\text{-}\eta^2\text{:}\eta^2\text{:}\eta^2\text{-arene})$.[6] All these crystals contain molecular "chains" in which adjacent arenes on neighboring molecules interact *via* graphitic-type interactions. The chains formed are either straight or zigzagged depending on the structure of the cluster, *i.e.* the angle between the two arene planes on the molecule.

® Abstract published in *Advance ACS Abstracts*, April 15, 1994.

(1) (a) Kitaigorodsky, A. I. In *Mixed Crystals*; Cardona, M., Ed.; Solid State Sciences, Vol. 33; Springer-Verlag: Berlin, 1984. (b) Bernstein, J. In *Organic Solid State Chemistry*; Desiraju, G. R., Ed.; Elsevier: Amsterdam, 1987; p 471. (c) Bernstein, J.; Hagler, A. T. *J. Am. Chem. Soc.* **1978**, *100*, 673. (d) *Structure and Properties of Molecular Crystals*; Pierrot, M., Ed.; Elsevier: Amsterdam, 1990. (e) Desiraju, G. R. *Crystal Engineering. The Design of Organic Solids*; Elsevier: Amsterdam, 1989.

(2) See, for example: (a) Braga, D.; Grepioni, F.; Milne, P.; Parisini, E. *J. Am. Chem. Soc.* **1993**, *115*, 5115. (b) Riley, P. E.; Davis, R. E. *Inorg. Chem.* **1976**, *15*, 2735. (c) Hunter, G.; Blount, J. F.; Damewood, J. R.; Iverson, D. J.; Mislow, K. *Organometallics* **1982**, *1*, 448. (d) Braga, D.; Grepioni, F. *Acc. Chem. Res.* **1994**, *27*, 51.

(3) Dyson, P. J.; Johnson, B. F. G.; Reed, D.; Braga, D.; Grepioni, F.; Parisini, E. *J. Chem. Soc., Dalton Trans.* **1993**, 2817.

(4) (a) Sirigu, A.; Bianchi, M.; Benedetti, E. *J. Chem. Soc., Chem. Commun.* **1969**, 596. (b) Braga, D.; Grepioni, F.; Dyson, P. J.; Johnson, B. F. G.; Frediani, P.; Bianchi, M.; Piacenti, F. *J. Chem. Soc., Dalton Trans.* **1992**, 2565.

(5) (a) Braga, D.; Grepioni, F.; Johnson, B. F. G.; Chen, H.; Lewis, J. *J. Chem. Soc., Dalton Trans.* **1991**, 2559. (b) Braga, D.; Grepioni, F.; Johnson, B. F. G.; Lewis, J.; Housecroft, C. E.; Martinelli, M. *Organometallics* **1991**, *10*, 1260.

(6) (a) Braga, D.; Dyson, P. J.; Grepioni, F.; Johnson, B. F. G. *Chem. Rev.*, in press. (b) Wadepohl, H. *Angew. Chem., Int. Ed. Engl.* **1992**, *31*, 247.

(7) Braga, D.; Grepioni, F.; Righi, S.; Dyson, P. J.; Johnson, B. F. G.; Bailey, P. J.; Lewis, J. *Organometallics* **1992**, *11*, 4042.

0276-7333/94/2313-2170$04.50/0

Results and Discussion

Synthesis and Chemical Characterization. Our usual technique for preparing bis(arene) derivatives, from mono(arene) starting materials $Ru_6C(CO)_{14}$(arene), involves the removal of two carbonyl groups by the oxidative decarbonylation reagent Me_3NO followed by addition of the appropriate dihydroarene, yielding compounds of formula $Ru_6C(CO)_{12}$(arene)(dihydroarene). Expulsion of a further CO group brings about the dehydrogenation of the ring, affording the bis(arene) cluster.

Due to problems encountered with the reduction of xylene to dihydroxylene, an alternative method was devised in which the cluster reacts directly with xylene. In this reaction the xylene species $Ru_6C(CO)_{14}(\eta^6\text{-}C_6H_4Me_2)$ (1) was treated with 3 molar equiv of Me_3NO, added dropwise in dichloromethane to a solution of 1 in dichloromethane–acetone–xylene. Acetone was added to stabilize any unsaturated cluster compounds produced in the course of the reaction. The mixture was allowed to stir for about 1 h at room temperature. Chromatographic separation on silica was then carried out, with dichloromethane–hexane (1:1, v/v) as eluent.

Initially, a major brown product was extracted and, after crystallization from dichloromethane, into which pentane diffused, the cocrystal **C** was produced. This crystal contains molecules of both the starting material $Ru_6C(CO)_{14}(\eta^6\text{-}C_6H_4Me_2)$ (1) and the desired product $Ru_6C(CO)_{11}(\eta^6\text{-}C_6H_4Me_2)_2$ (2). Although this was unintentional, we have since been able to separate the two species using a different eluent, dichloromethane–hexane–ethyl acetate (3:1:17, v/v) and have obtained a structure of the new species **2**, **1** having been reported previously in the crystal **A**. Mixing equimolar amounts of the two clusters **1** and **2** in the same crystallizing medium used before, we obtained the identical cocrystals **C**. Complex **2** has also been separately crystallized and characterized by X-ray diffraction in its homomolecular crystalline form **B**. The relationship between molecular and crystalline forms is summarized in the following table:

complex	species	homomolecular crystal	heteromolecular crystal
$Ru_6C(CO)_{14}(\eta^6\text{-}C_6H_4Me_2)$	1	A	C
$Ru_6C(CO)_{11}(\eta^6\text{-}C_6H_4Me_2)_2$	2	B	C

When required in the following discussion, the symbols **1(A)**, **2(B)**, **1(C)**, and **2(C)** will also be used to designate the individual molecules in the corresponding crystals.

While complex **1** has been reported before,[3] the bis(xylene) species **2** is new. Characterization of **2** has also been established spectroscopically, and these findings are concurrent with the X-ray structure. The mass spectrum shows a strong parent peak at 1137 (calculated = 1139), followed by the loss of five carbonyl groups in succession. The fragmentation pattern becomes too complicated to observe the loss of any other groups, or recognize any specific cluster fragments. The ^1H NMR also indicates the presence of two chemically equivalent η^6-xylene ligands. Signals are observed at δ 5.53 (1H, t, J = 1.2 Hz), 5.32 (1H, t, J = 6 Hz), 5.13 (2H, d of d, J = 6 Hz, 1.2 Hz), and 2.15 (6H, s). Due to the small coupling constant the triplet at δ 5.53 ppm can be assigned to the ring proton situated between the two methyl groups, while the other triplet with the much larger coupling constant must arise from the proton on the opposite carbon atom. The other signal at δ 5.13 ppm shows coupling to both these former signals, and since it has a relative intensity of 2, must be derived from the two remaining aromatic protons, which would be expected to be equivalent. Lastly, the methyl groups give rise to the singlet at δ 2.15 ppm.

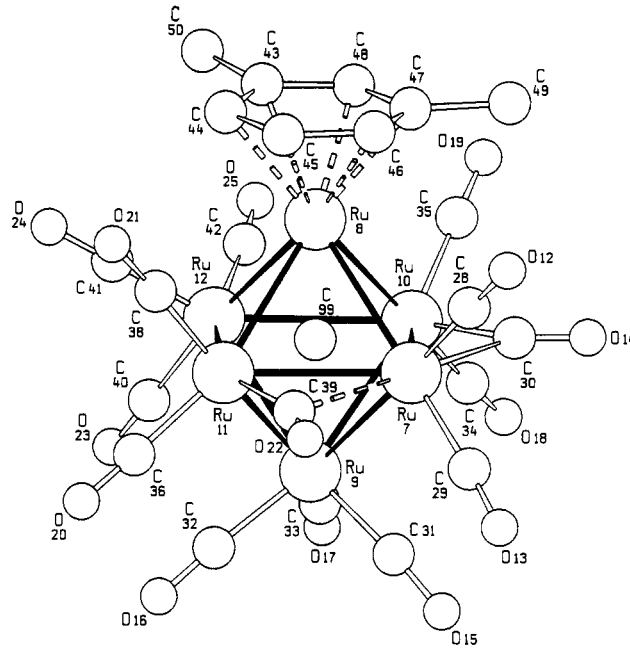

Figure 1. Molecular structure of **1** as determined in its crystal form **C**. Hydrogen atoms are omitted for clarity.

Molecular Structures of 1 and 2. The complexes **1(A)**, **2(B)**, **1(C)**, and **2(C)** possess structural features that are common to most mono- and bis(arene) hexaruthenium clusters. The molecular structure of species **1** in its novel crystal form **C** is shown in Figure 1. Analogously, the molecular structure of **2** in the crystal form **B** and **C** is shown in Figure 2 together with the relative labeling schemes. Relevant structural parameters for **1(C)** and **2(C)** are reported in Table 1; those for species **2(B)** are listed in Table 2. The most relevant structural features of the two complexes in the two crystals can be summarized as follows:

(i) The cluster core, as in the parent molecule $Ru_6C(CO)_{17}$,[4] is constituted of an octahedral metal atom framework encapsulating the interstitial C(carbide) atom.

(ii) In both **1** and **2** the xylene ligands are terminally bound to the metal cluster, formally replacing three carbon monoxide ligands on each coordination site.

(iii) The molecular equators contain one symmetric bridging CO spanning one Ru–Ru edge and two bent terminal ligands; all remaining CO's are terminally bound, the CO ligand distribution is thus reminiscent of that observed in $Ru_6C(CO)_{17}$ and in most of its derivatives.

(iv) The interstitial C(carbide) atom in **1(C)** shows a "drift" toward the arene bound apex [C(99)–Ru(8) 1.91(2) *vs* an average of 2.06(2) Å for the remaining C(99)–Ru bond distances.

(v) In **2(B)** and **2(C)** the whole octahedron appears to be contracted along the arene coordination axis with average short and long Ru–C(carbide) bond distances of 1.98(1) *vs* 2.06(1) Å and 1.96(2) *vs* 2.07(2) Å, for **2(B)** and **2(C)**, respectively.

In addition to these general features, it is worth pointing out that the conformation of the xylene ligand in **1(C)** (see Figure 3c) is similar to that observed for *one* of the two independent molecules present in the asymmetric unit

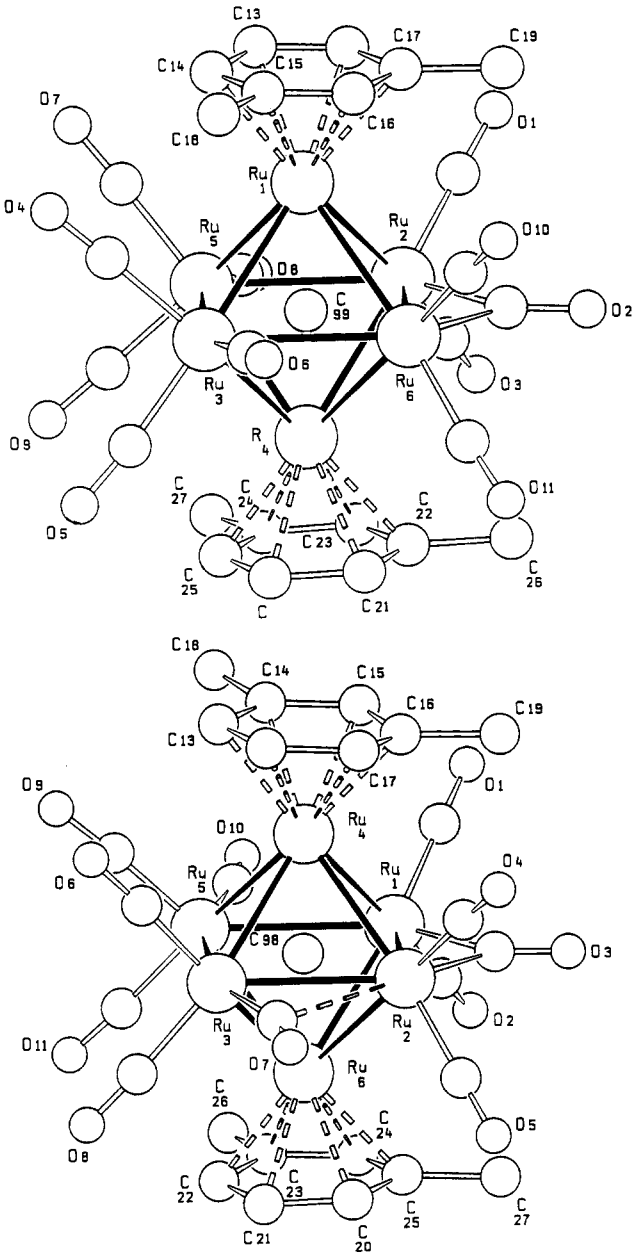

Figure 2. Molecular structure of **2** as determined in its crystal form **B** (a, top) and **C** (b, bottom). Hydrogen atoms are omitted for clarity, the C atoms of the CO ligands carry the same labeling as the corresponding O atoms.

of the homomolecular crystal of $Ru_6C(CO)_{14}(\eta^6\text{-}C_6H_4Me_2)$, **1(A)** (see Figure 3a,b). Furthermore the C_6 rings and one of the methyl groups of the two xylene ligands in **2(B)** are eclipsed, while the remaining two methyl groups form an angle of *ca.* 120° in projection (see Figure 3d). In molecule **2(C)**, on the other hand, the two xylene ligands are eclipsed (see Figure 3e). These features are in keeping with the conformational *nonpreference* generally shown by η^6-bound arenes in the family of pentanuclear and hexanuclear arene clusters of ruthenium. This nonpreference has been taken as indicative of the absence of well-defined minima in the conformational potential energy surface for apically bound arenes. This is also in agreement with the observation of three different relative orientations of the apical tricarbonyl units in the solid state structure of the parent binary carbonyl $Ru_6C(CO)_{17}$.[4b]

Crystal Structures of Crystals B and C. The observed crystal structures have been *decoded* by employing methods previously applied to the investigation of the intermolecular interlocking and crystalline organization in a number of organometallic crystals.[4,5] We focus our attention on the distribution and interaction of the first-neighboring molecules among the molecules surrounding the one chosen as reference in order to achieve an accurate knowledge of the immediate molecular environment and of molecular organization in the crystal structure. Empirical packing potential energy calculations within the pairwise atom–atom approach and packing analysis based on graphical methods are used to this purpose. The packing potential energy of an organometallic molecule (ppe) can be estimated by applying atom–atom pairwise potential energy calculations similar to those usually employed in the neighboring field of solid state organic chemistry[8] (see Experimental Section).

Table 1. Selected Bond Lengths (Å) and Angles (deg) for 1(C) and 2(C)

		Compound **1(C)**	
Ru(1)–Ru(2)	2.857(2)	Ru(4)–C(12)	2.22(2)
Ru(1)–Ru(4)	2.842(2)	Ru(4)–C(13)	2.22(2)
Ru(1)–Ru(5)	3.040(3)	Ru(4)–C(14)	2.24(2)
Ru(1)–Ru(6)	2.835(3)	Ru(4)–C(15)	2.27(2)
Ru(2)–Ru(3)	2.941(3)	Ru(4)–C(16)	2.21(2)
Ru(2)–Ru(4)	2.854(3)	Ru(4)–C(17)	2.24(3)
Ru(2)–Ru(6)	2.849(3)	C(12)–C(13)	1.44(3)
Ru(3)–Ru(4)	2.855(3)	C(12)–C(17)	1.44(4)
Ru(3)–Ru(5)	2.819(3)	C(13)–C(14)	1.40(4)
Ru(3)–Ru(6)	2.841(2)	C(14)–C(15)	1.45(4)
Ru(4)–Ru(5)	2.828(3)	C(14)–C(18)	1.51(4)
Ru(5)–Ru(6)	2.852(3)	C(15)–C(16)	1.37(3)
Ru(1)–C(98)	2.07(1)	C(16)–C(17)	1.33(4)
Ru(2)–C(98)	2.07(2)	C(16)–C(19)	1.53(3)
Ru(3)–C(98)	2.06(1)	Ru(6)–C(20)	2.23(2)
Ru(4)–C(98)	1.97(2)	Ru(6)–C(21)	2.23(2)
Ru(5)–C(98)	2.06(2)	Ru(6)–C(22)	2.22(2)
Ru(6)–C(98)	1.95(2)	Ru(6)–C(23)	2.24(2)
Ru–C (mean)	1.88(2)	Ru(6)–C(24)	2.23(2)
C–O (mean)	1.14(3)	Ru(6)–C(25)	2.25(2)
Ru(1)–C(3)	2.04(3)	C(20)–C(21)	1.38(3)
Ru(2)–C(3)	2.06(2)	C(20)–C(25)	1.36(3)
Ru(3)–C(7)	1.95(2)	C(21)–C(22)	1.45(3)
Ru(2)···C(7)	2.75(2)	C(22)–C(23)	1.40(3)
		C(23)–C(24)	1.40(3)
		C(23)–C(26)	1.46(3)
		C(24)–C(25)	1.44(3)
		C(25)–C(27)	1.53(4)
O–C–Ru (mean)	176(2)	O(7)–C(7)–Ru(3)	162(2)
O(3)–C(3)–Ru(1)	137(2)	O(7)–C(7)–Ru(2)	123(2)
O(3)–C(3)–Ru(2)	135(2)		
		Compound **2(C)**	
Ru(7)–Ru(8)	2.885(2)	Ru–C (mean)	1.88(3)
Ru(7)–Ru(9)	2.941(3)	C–O (mean)	1.15(3)
Ru(7)–Ru(10)	2.845(2)	Ru(7)–C(30)	2.20(2)
Ru(7)–Ru(11)	2.869(3)	Ru(7)···C(38)	2.47(3)
Ru(8)–Ru(10)	2.870(2)	Ru(10)–C(30)	2.04(2)
Ru(8)–Ru(11)	2.870(3)	Ru(11)–C(38)	1.95(3)
Ru(8)–Ru(12)	2.845(3)	Ru(8)–C(42)	2.27(2)
Ru(9)–Ru(10)	2.849(3)	Ru(8)–C(43)	2.22(2)
Ru(9)–Ru(11)	2.889(3)	Ru(8)–C(44)	2.22(2)
Ru(9)–Ru(12)	2.834(2)	Ru(8)–C(45)	2.22(2)
Ru(10)–Ru(12)	3.020(3)	Ru(8)–C(46)	2.25(2)
Ru(11)–Ru(12)	2.894(3)	Ru(8)–C(47)	2.22(2)
Ru(7)–C(99)	2.07(2)	C(42)–C(43)	1.36(3)
Ru(8)–C(99)	1.91(2)	C(42)–C(47)	1.40(3)
Ru(9)–C(99)	2.10(2)	C(42)–C(49)	1.58(4)
Ru(10)–C(99)	2.03(2)	C(43)–C(44)	1.45(3)
Ru(11)–C(99)	2.07(2)	C(44)–C(45)	1.39(3)
Ru(12)–C(99)	2.05(2)	C(45)–C(46)	1.40(3)
		C(46)–C(47)	1.39(3)
		C(46)–C(48)	1.51(3)
O–C–Ru (mean)	176(2)	O(22)–C(38)–Ru(11)	156(3)
O(14)–C(30)–Ru(7)	133(2)	O(22)–C(38)–Ru(7)	124(2)
O(14)–C(30)–Ru(10)	142(2)		

Table 2. Selected Bond Lengths (Å) and Angles (deg) for 2(B)

Ru(1)–Ru(2)	2.8625(13)	Ru(1)–C(15)	2.289(12)
Ru(1)–Ru(3)	2.8425(14)	Ru(1)–C(16)	2.233(10)
Ru(1)–Ru(5)	2.8619(13)	Ru(1)–C(17)	2.254(12)
Ru(1)–Ru(6)	2.8553(14)	C(12)–C(13)	1.37(2)
Ru(2)–Ru(4)	2.8478(14)	C(12)–C(17)	1.40(2)
Ru(2)–Ru(5)	2.9770(14)	C(13)–C(14)	1.45(2)
Ru(2)–Ru(6)	2.849(2)	C(14)–C(15)	1.40(2)
Ru(3)–Ru(4)	2.8482(13)	C(15)–C(16)	1.34(2)
Ru(3)–Ru(5)	2.8071(14)	C(15)–C(18)	1.51(2)
Ru(3)–Ru(6)	3.018(2)	C(16)–C(17)	1.46(2)
Ru(4)–Ru(5)	2.8370(13)	C(17)–C(19)	1.49(2)
Ru(4)–Ru(6)	2.8522(13)	Ru(4)–C(20)	2.248(12)
Ru(1)–C(99)	1.985(12)	Ru(4)–C(21)	2.258(12)
Ru(2)–C(99)	2.059(13)	Ru(4)–C(22)	2.257(12)
Ru(3)–C(99)	2.062(13)	Ru(4)–C(23)	2.268(13)
Ru(4)–C(99)	1.956(12)	Ru(4)–C(24)	2.318(11)
Ru(5)–C(99)	2.083(11)	Ru(4)–C(25)	2.211(13)
Ru(6)–C(99)	2.040(11)	C(20)–C(21)	1.41(2)
Ru–C (mean)	1.891(13)	C(20)–C(25)	1.37(2)
C–O (mean)	1.13(2)	C(21)–C(22)	1.36(2)
Ru(2)–C(2)	2.053(15)	C(22)–C(23)	1.44(2)
Ru(6)–C(2)	2.037(12)	C(22)–C(26)	1.52(2)
C(2)–O(2)	1.20(2)	C(23)–C(24)	1.40(2)
Ru(1)–C(12)	2.224(11)	C(24)–C(25)	1.46(2)
Ru(1)–C(13)	2.221(10)	C(24)–C(27)	1.48(2)
Ru(1)–C(14)	2.216(12)		
O–C–Ru (mean)	175.6(12)	O(2)–C(2)–Ru(2)	136.7(12)
O(2)–C(2)–Ru(6)	134.9(13)		

The efficiency of volume occupation in the crystal can be evaluated by estimating the packing coefficients (pc) from the relationship pc = $V_{mol}Z/V_{cell}$, where V_{mol} represents the van der Waals molecular volume. These volumes have been estimated with the integration method put forward by Gavezzotti.

The heteromolecular crystal **C** formed by cocrystallization of **1** and **2** can be described as being constituted of an alternating stack of *bimolecular layers* each formed of molecules of the same type. The bimolecular layers of **1** and **2** are schematically represented in Figure 4. Each bimolecular layer is effectively a tridimensional crystal on its own. The bimolecular layer of **1(C)** contains molecules of type 1, arranged in piles, with the xylene of each molecule interlocked with the tricarbonyl unit of a next neighboring molecule along the pile (see Figure 5a). This is exactly the same packing motif observed in crystalline **1(A)** (see Figure 5b) and is similar to that shown by other mono(arene) derivatives of $Ru_6C(CO)_{17}$.[6] The bimolecular layers of **2(C)** are formed by molecular piles (see Figure 6a) based on the quasi face-to-face interaction between next neighboring xylenes with an interarene separation of *ca.* 3.4 Å. Remarkably, this is also the fundamental packing motif present in the homomolecular crystal **2(B)** (see Figure 6b), although in this crystal the relative conformation of the xylene ligands facing each other along the pile permits a better superimposition than in the cocrystal. This packing motif is reminiscent of that observed in the bis(arene) species *trans*-$Ru_6C(CO)_{11}(\eta^6\text{-}C_6H_3Me_3)_2$[9a] and *trans*-$Ru_6C(CO)_{11}(\eta^6\text{-}C_6H_6)_2$.[9b]

All crystal structure parameters relevant for the following discussion are grouped in Table 3 which allows the following general observations to be made.

(i) The molecular volumes, calculated with the integration method (see Experimental Section), for the three molecules of **1** and for the two molecules of **2**, have strictly comparable values within the two sets. This indicates that neither the rotameric conformation of the xylene ligands nor the different crystalline environments affect the van der Waals volumes to any appreciable extent.

(ii) The two types of potential parameters yield values of the packing potential energy and of the molecule–molecule interactions which are numerically different; in general the GVF parameters yield more cohesive crystals. These differences, however, are of little significance because of the severe approximations and assumptions required to estimate atom–atom packing potential energies in the case of high nuclearity metal cluster molecules. Empirical calculations of the type employed in this work can only be used on a *relative basis* to compare closely related species.

(iii) On the other hand the two sets of parameters rank the crystal energies and the intermolecular interactions in the same way. This is an important indication that, although the actual values of the cohesive energies may not be reliable, the differences in energy appear to be physically meaningful and can thus lead to some useful considerations.

(iv) The interaction between the two independent molecules in the unit cell of crystal **A** [**1(A)–1(A)′**] contributes about 10% more than any other intermolecular pairwise interactions and is, therefore, the most cohesive molecule–molecule interaction in crystal **A**.

(v) Irrespective of the potential parameters choice, the interaction **1(A)–1(A)′** is also stronger than the strongest molecule–molecule interaction in **B** [**2(B)–2(B)**] and of the heteromolecular interaction in crystal **C** [**1(C)–2(C)**]. This could be surprising at first, because molecules of type **2** contain "more atoms" than molecules of type 1 and should, therefore, be favored by the atom–atom potential energy. This being not the case, one has to invoke a more efficient intermolecular interlocking between mono(xylene) rotamers with respect to bis(xylene) clusters to explain the observation. In keeping with this, the heteromolecular interaction **1–2** in crystal **C** is almost identical in pairwise energy to the homomolecular interactions in crystal **B**.

(vi) The three crystals **A–C** possess essentially the same values of the ppe as well as identical packing coefficients [0.72]. Hence, the cocrystal and the two homomolecular crystals are strictly comparable in terms of cohesive energies and efficiency of volume occupation. This is an important insight into the specific cocrystallization phenomenon that we are discussing herein, yielding a firm indication that the cocrystal can be obtained so easily only because it is competitive with the two separate crystals. Although considerations on the entropic contribution to crystallization phenomena should be made with great caution it is very reasonable to presume that the cocrystallization will be entropically favored over the separation into homomolecular crystals.

In summary the cocrystal of **1** and **2** can be regarded as composed of homomolecular crystals of **1** and of homomolecular crystals of **2**, both extending for only two layers. This, of course, is only a means to describe the *crystal*

(8) (a) Kitaigorodsky, A. I. *Molecular Crystals and Molecules*; Academic Press: New York, 1973. (b) Gavezzotti, A.; Simonetta, M. *Chem. Rev.* **1981**, *82*, 1. (c) *Organic Solid Chemistry*; Desiraju, G. R., Ed.; Elsevier: Amsterdam, 1987. (d) Dauber, P.; Hagler, A. T. *Acc. Chem. Res.* **1980**, *13*, 105.

(9) (a) Braga, D.; Grepioni, F.; Righi, S.; Johnson, B. F. G.; Bailey, P. J.; Dyson, P. J.; Lewis, J.; Martinelli, M. *J. Chem. Soc., Dalton Trans.* **1992**, 2121. (b) Adams, R. D.; Wu, W. *Polyhedron* **1992**, *2*, 2123.

(10) Braga, D.; Grepioni, F.; Parisini, E.; Dyson, P. J.; Johnson, B. F. G.; Reed, D.; Shepherd, D. S.; Bailey, P. J.; Lewis, J. *J. Organomet. Chem.* **1993**, *462*, 301.

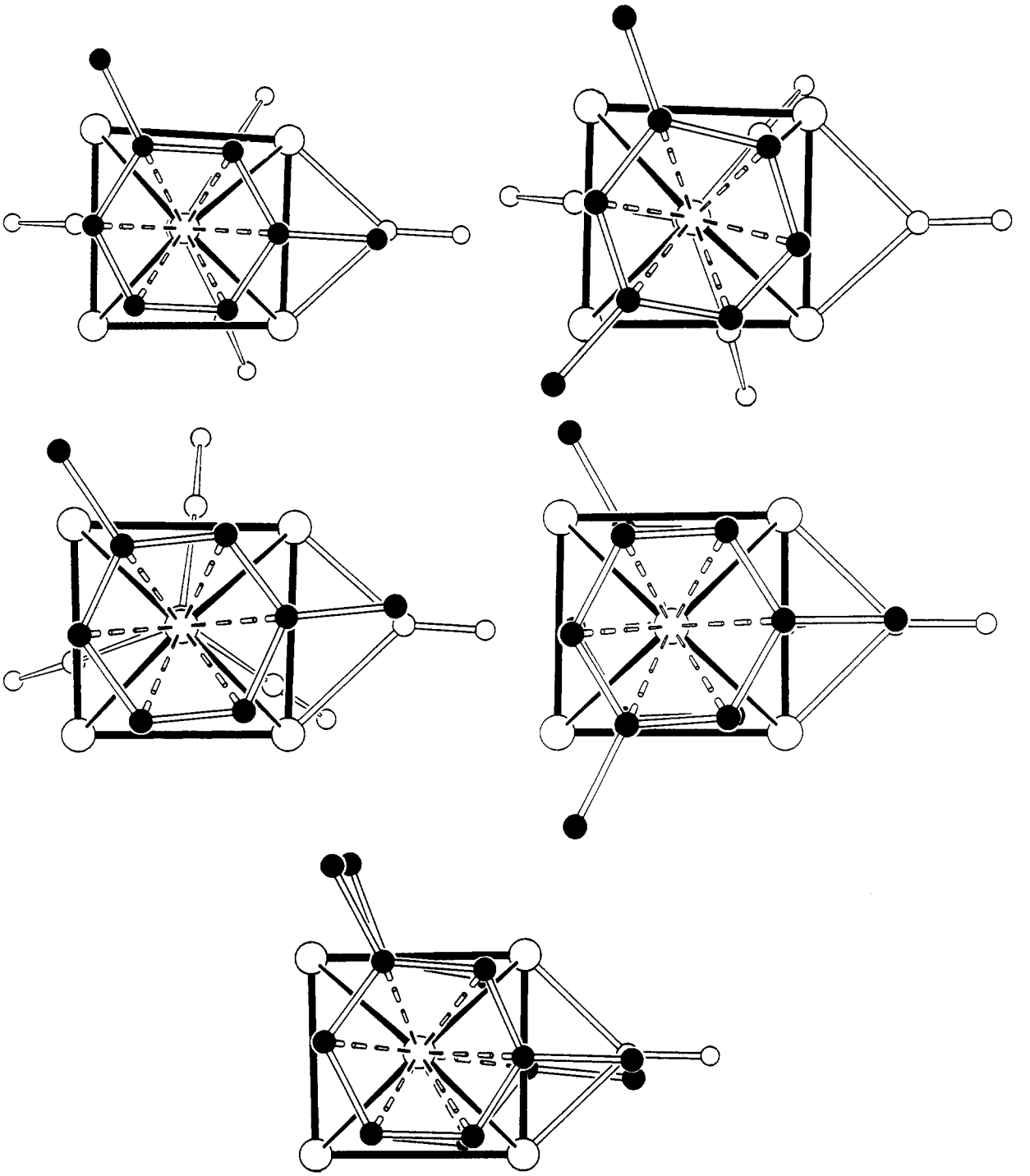

Figure 3. Schematic representation of the different conformations of the xylene ligand in the two independent molecules of 1 present in crystal **A** (a and b, top left and right), and in molecule **1(C)** (c, middle left). Comparison of the relative conformations of the xylene ligands in molecules **2(B)** (d, middle right) and **2(C)** (e, bottom).

structure of the cocrystal and to rationalize differences and similarities between the hetero- and homomolecular crystals and carries no direct implication on the actual nucleation or growth processes behind the construction of the heteromolecular crystal.

Concluding Remarks

Mono- and bis(arene) derivatives of $Ru_6C(CO)_{17}$ now form a well established class of organometallic cluster complexes. These molecules show a great structural variability thanks mainly to the availability of different coordination sites over the cluster framework for the apically bound ligands, to the different bonding modes that the arenes can adopt, and to the conformational freedom that the arene(s) possess when apically bound. Evidence that the arene ligands are free to rotate is shown by NMR spectra in which,[10] for example, protons of benzene exhibit a singlet, thereby sharing the same chemical environment. Under these conditions it is very likely that different rotamers are cocrystallized. This results in the presence of more than one independent molecule in the unit cell.[11] This phenomenon is more often encountered when the symmetry of the arene ligand is low, as happens with xylene or toluene. Other examples are afforded by the crystals of the mixed-arene species

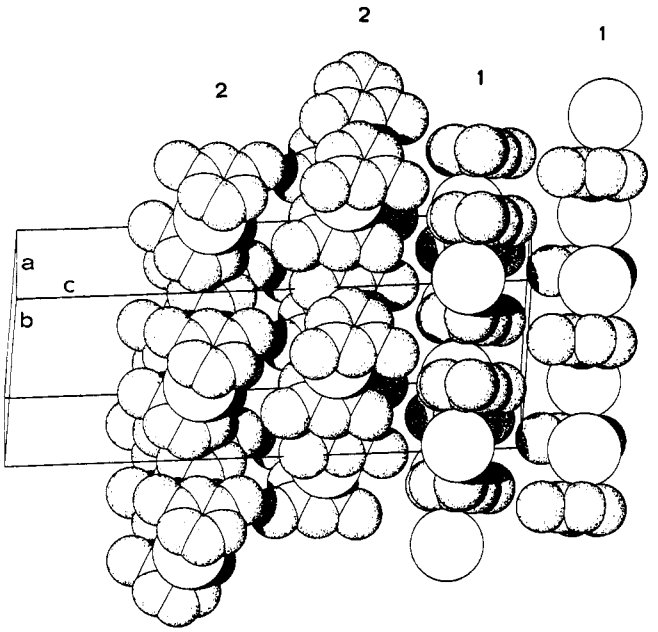

Figure 4. Schematic representation of the layered structure of crystal **C** composed of bimolecular layers of molecules **1** and **2**. The CO ligands and the hydrogen atoms are omitted for the sake of clarity, the large spheres represent the cluster cores.

$Ru_6C(CO)_{11}(\eta^6$-xylene)(η^6-benzene) and $Ru_6C(CO)_{11}(\eta^6$-xylene)(η^6-toluene). Crystals containing different isomeric forms of the same molecules can thus be regarded as pseudococrystals.

The rationalization of the cocrystallization phenomenon described in this report is not easy. First one has to understand why a molecular layer formed by one type of molecule "prefers" to interact on one side with another molecular layer of the same type and on the opposite side with molecules of the other type.

Crystalline arene clusters have been shown to pack according to only a few, well-defined, packing motifs. These are dictated by the need to optimize the intermolecular interlocking of flat arene fragments and of cylindrical carbonyl ligands. It has been demonstrated that organometallic clusters form essentially molecular crystals, *viz.* crystals held together by van der Waals type interactions of the type commonly observed in organic solids. The relationship between the molecular and crystal structure for this class of complexes still poses a number of intriguing (and fascinating) problems. The understanding of this relationship is essential to the growth of the solid state chemistry of organometallic molecules as it has been (and still is) in the more mature neighboring field of solid state organic chemistry.

Experimental Section

Synthesis and Spectroscopic Characterization of $Ru_6C(CO)_{14}(\eta^6$-$C_6H_4Me_2)$ from $Ru_6C(CO)_{14}(\eta^6$-$C_6H_4Me_2)$. All reactions were carried out with the exclusion of air and moisture, using a nitrogen atmosphere and freshly distilled solvents. Subsequent workup of the products was achieved without precautions to exclude air using standard laboratory grade solvents. Infrared spectra were recorded on a Perkin-Elmer 1600 Series FTIR in CH_2Cl_2 using NaCl cells. Positive fast atom bombardment mass spectra were obtained using a Kratos MS50TC spectrometer, with CsI as calibrant. ^{1}H NMR spectra were recorded in $CDCl_3$ using a Bruker AM360 instrument, referenced to internal TMS. Thin layer chromatography (TLC) was carried out on plates supplied by Merck coated with a 0.25-mm layer of Kieselgel 60 F_{254}. $Ru_6C(CO)_{14}(\eta^6$-$C_6H_4Me_2)$ was prepared according to the literature procedure.[3] Trimethylamine *N*-oxide (Me_3NO) was sublimed prior to reaction.

$Ru_6C(CO)_{14}(\eta^6$-$C_6H_4Me_2)$ (**1**) (110 mg) was dissolved in a solution of dichloromethane (40 mL), xylene (10 mL), and acetone (5 mL). To this solution, was added Me_3NO (3.3 molar equiv, 24 mg) dropwise in dichloromethane (10 mL) and acetone (5 mL). The reaction mixture was stirred for a total period of 1 h, after which IR spectroscopy indicated a significant change had occured. The reaction mixture was filtered, the solvent was removed *in vacuo*, and the residues were redissolved in a minimum amount of dichloromethane. The products were then separated by TLC with dichloromethane–hexane–ethyl acetate (3:1:17, v/v) as eluent. In order of elution two brown bands were extracted and characterized as the new material $Ru_6C(CO)_{11}(\eta^6$-$C_6H_4Me_2)_2$ (**2**) (21 mg) and the starting material $Ru_6C(CO)_{14}(\eta^6$-$C_6H_4Me_2)$ (**1**) (25 mg).

The homomolecular crystals of **2(B)** were grown from a solution

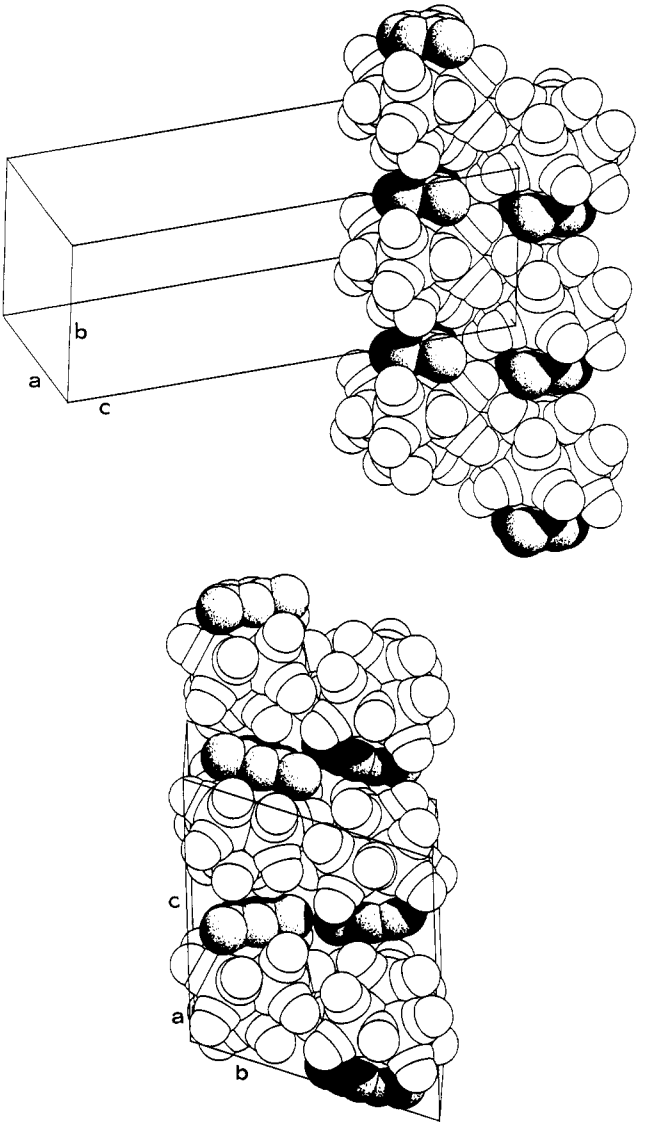

Figure 5. (a, Top) bimolecular layer of **1(C)** containing molecules arranged in piles with the xylene of each molecule interlocked with the tricarbonyl unit of a next neighboring molecule along the pile. Compare this with the packing motif observed in crystalline **1(A)** (b, bottom).

(11) One may wonder why two such independent molecules are more often present than three or more. One should keep in mind, however, that very large unit cells are often looked at with suspicion by the crystallographer; besides they are often beyond the resolution power of routine diffractometers. Data in these cases are not collected.

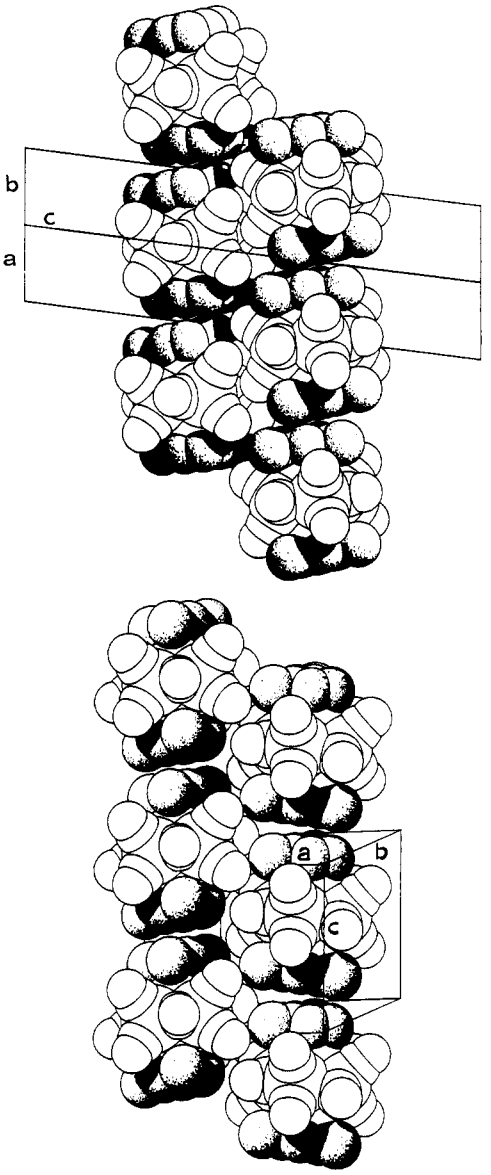

Figure 6. Bimolecular layer of **2(C)** formed by molecular piles based on the quasi face-to-face interaction between next neighboring xylenes (a, top). Compare this with the packing motif present in the homomolecular crystal **2(B)** (b, bottom).

of dichloromethane, into which pentane was diffused. The cocrystal system **C** was nucleated by the same method, but from an equimolar mixture of compounds **1** and **2**.

Structural Characterization. Crystal data and details of measurements for compounds **1** and **2** in the crystalline forms **B** and **C** are summarized in Table 4. Diffraction intensities were collected at room temperature on an Enraf-Nonius CAD-4 diffractometer equipped with a graphite monochromator (Mo Kα, λ = 0.710 69 Å). Intensities data were reduced to F_o^2. The structures were solved by direct methods followed by least-squares refinements. For all calculations the crystallographic programs SHELX86[12a] and SHELXL93[12b] were used. Crystal **C** was not stable under X-ray exposure, showing a decay of *ca.* 30% of the control intensities over the long period of data collection. The diffraction data were corrected for decay, but an empirical absorption correction was not possible. Altogether the diffraction data for crystal **C** are slightly poorer than those obtained for **B** (see agreement indices in Table 4). All non-hydrogen atoms in both compounds were allowed to vibrate anisotropically with the exception of two C atoms and one O atom in **1(C)**, which yielded nonpositive definite ellipsoids and were treated isotropically. The hydrogen atoms were added in calculated positions [C_{sp^2}–H 0.93, C_{sp^3}–H 0.96 Å] and refined "riding" on the corresponding C atoms. Fractional atomic coordinates of **2(B)** and **1(C)–2(C)** are deposited as supplementary material. For structural representation the molecular graphic program SCHAKAL92[13] was used.

Packing Potential Energy Calculations. Packing potential energy calculations were performed within the atom–atom pairwise potential energy method. Use is made of the expression ppe = $\sum_i \sum_j [A \exp(-Br_{ij}) - Cr_{ij}^{-6}]$, where ppe represents the packing

Table 3. Comparison of Relevant Crystal Packing Parameters

	1 crystal **A**	**2** crystal **B**	**1** and **2** crystal **C**
	space group $P\bar{1}$, $Z = 2$	space group Pn, $Z = 2$	space group $P\bar{1}$, $Z = 2.2^c$
V_{cell} (Å^3)	2827.4	1553.6	2981.2
V_{mol} (Å^3)	510.1, 510.2[a]	561.6	mono: 509.2 bis: 559.4
packing coeff	0.72	0.72	0.72
mol1–mol2 MRK (kcal·mol^{-1})	−13.0	−11.6	−11.9
mol1–mol2 GVF (kcal·mol^{-1})	−15.0	−13.8	−13.7
ppe MRK (kcal·mol^{-1})	−92.4[a]	−94.2	mean: −93.1[b]
ppe GVF (kcal·mol^{-1})	−110.9[a]	−112.0	mean: −111.3[b]

[a] Mean value averaged over the two independent molecules present in the unit cell. [b] A sort of mean packing potential energy value averaged over the two different molecules; MRK and GVF indicate the two types of atom–atom potential parameters used in the calculations (see Experimental Section). [c] **1(C)** and **2(C)** are present with two molecules each in the unit cell.

Table 4. Crystal Data and Details of Measurements for 2(B) and 1(C)–2(C)

	2(B)	**1(C)–2(C)**
formula	$C_{28}H_{20}O_{11}Ru_6$	$C_{23}H_{10}O_{14}Ru_6 \cdot C_{28}H_{20}O_{11}Ru_6$
mol wt	1138.86	1127.80
temp (K)	293	293
syst	monoclinic	triclinic
space group	Pn	$P\bar{1}$
a (Å)	10.242(3)	9.852(4)
b (Å)	14.047(6)	10.444(9)
c (Å)	11.242(2)	32.320(10)
α (deg)	90.0	95.65(5)
β (deg)	106.15(2)	92.03(4)
γ (deg)	90.0	115.29 (4)
V (Å^3)	1553.6(9)	2981(3)
Z	2	2c, 2[a]
F(000)	1080	2128
λ(Mo Kα) (Å)	0.710 69	0.710 69
μ(Mo Kα) (mm^{-1})	2.669	2.784
θ range (deg)	3–25	3–25
ω-scan width (deg)	0.70	1.30
octants explored (h_{min}, h_{max}; k_{min}, k_{max}; l_{min}, l_{max})	−12, 11; 0, 16; 0, 13	−11, 11; −12, 12; 0, 31
measd reflns	3005	9915
no. of unique reflns	2879	9711
no. of refined params	406	773
GOF on F^2	1.134	1.196
R_1 (on F, $I > 2\sigma(I)$)	0.0416	0.0807
wR_2 (on F^2)	0.1045	0.2388

[a] Two molecules of **1(C)** and **2(C)**, respectively, are present in the unit cell.

(12) (a) Sheldrick, G. M. *Acta Crystallogr.* **1990**, *A46*, 467. (b) Sheldrick, G. M. SHELXL93. University of Gottingen, 1993.

(13) Keller, E. SCHAKAL92; Graphical Representation of Molecular Models. University of Freiburg, RFG.

potential energy and r_{ij} is the nonbonded atom–atom intermolecular distance. Index i in the summation runs over all atoms of the reference molecule and index j over the atoms of the surrounding molecules or ions within a preset cutoff distance (usually 15 Å with large cluster systems). The ruthenium atoms were attributed the potential coefficients available for argon. Two sets of potential parameters have been used for carbon and oxygen: the generalized potential energy parameters obtained by Gavezzotti and Filippini[14a] (set GVF in the supplementary table) and those of Mirsky (set MRK).[14b] Mirsky's parameters have also been used for the hydrogen atoms. These parameters are reported in the supplementary material. By this method the first coordination sphere around the molecule chosen for reference can be easily investigated and preferential packing motifs detected. The molecular volumes were calculated by using literature van der Waals radii for main-group elements (1.75, 1.50, and 1.17 Å for the C, O, and H atoms) and an arbitrary radius of 2.35 Å for the ruthenium atoms. The calculation procedures of V_{mol} and pc as well as that of ppe, are all implemented within Gavezzotti's OPEC suite of programs.[14c]

(14) (a) Mirsky, K. *Procedings of the International Summer School on Crystallographic Computing*; Delft University Press: Twente, The Netherlands, 1978; p 169. (b) Gavezzotti, A. OPEC. University of Milano, 1983. (c) Gavezzotti, A. *J. Am. Chem. Soc.* **1983**, *195*, 5220.

Acknowledgment. Financial support by MURST (D.B., F.G.), SERC, and British Petroleum (P.J.D.) and the ERAMUS exchange project "Crystallography" (C.M.) are acknowledged. D.B., F.G., and B.F.G.J. thank NATO for a travel grant.

Supplementary Material Available: For species **1** and **2** in their crystal forms **B** and **C**, tables of fractional atomic coordinates, anisotropic displacement parameters, fractional coordinates for the hydrogen atoms, and complete bonds and angles and a table of atom–atom potential energy parameters used in packing potential energy calculations (23 pages). Ordering information is given on any current masthead page.

OM930747G